Hydraulic Model Prediction of the Total Load of Sediment Transport in The Euphrates River at The Upstream Ramadi Barrage

Abdulhaleem A. Hammad[1,a *] and Sadeq O. Sulaiman[1,b]

[1] Dams and Water Resources Engineering Department, University of Anbar, Ramadi, Iraq.

[a]abd21e4002@uoanbar.edu.iq and [b]sadeq.sulaiman@uoanbar.edu.iq

*Corresponding author

Abstract. Examining river engineering properties and bed erosion is one of the most challenging but crucial issues in river engineering and sediment hydraulics, so preventing erosion and sedimentation is one of the primary goals of river management and prediction of river behavior. This research aims to give hydraulic engineers and decision-makers an accurate and dependable sediment transport equation that could be utilized to govern river engineering and modify river morphology. This study evaluated the carried sediments and their estimated quantity upstream of the Ramadi Barrage on the Euphrates River in the Anbar area of western Iraq. Six formulas, including Yang, Shen, Hung, Ackers and White, Engelund and Hansen, and Bagnold's and Toffaleti's, were used to evaluate the applicability of sediment transport in the study area. The performance of these models was assessed based on the precision of the actual sediment load relative to a specified deviation ratio. The analyses indicated that the Engelund-Hansen formula is the most applicable for this section of the river; that concludes, field data indicated an annual total sediment flow of roughly 1,536,337 tons.

Keywords: Bed load, empirical equations, Euphrates River, sediment transport, suspended load.

1. INTRODUCTION

Understanding river conditions, such as erosion and sedimentation, is a priority in engineering projects since rivers are an important water source for many uses. As a dynamic system, the river is constantly changing. The river also functions as a self-regulatory system since it modifies its properties in response to environmental changes. The changes in the environment could be the result of artificial activities like damming, river training, river diversion channelization, bank protection, and bridge and highway construction, or they could be the result of natural changes brought on by climate change, such as variations in vegetation cover[1]. Sediment accumulation and movement result in numerous issues. The channel's bed deforms more due to erosion and deposition of solid material on its banks and bed, affecting the waterway's ability to function hydraulically or for navigation. However, the deposit of materials raises the river bed, thereby expanding the flood range. Large quantities of money must, therefore, be spent on keeping the river's course appropriate for the hydraulic requirements. Thousands of tons of sediment are carried by rivers each year in various sizes and types of deposits, including coarse, soft, stone, sand, clay, and silt, each with its own set of characteristics[2,3]. Hydraulic characteristics, such as water velocity, flow, depth, and other control aspects, impact the amount and volume of these deposits and the river's ability to transport them. Particularly, hydraulic structures change a river's natural flow. For instance, a hydroelectric power plant's or weir's higher flow velocity causes the river bed's sediment to be subjected to more force, increasing the erosion rate. Additionally, sediment is deposited upstream of the structure, leaving a resource deficiency downstream[4]. Since a large portion of the sediment load comes from the channel's bottom and sides, rivers that flow through soft material often have higher sediment loads than rivers exposed to bedrock[5,6].

The effects of bed load and suspended sediment transport on aquatic life and water quality are one of the main problems in managing water resources[7]. Additionally, most building projects near or in the watercourse can potentially lessen nearby riverbanks' stability and increase suspended sediment and bed load transit. Most equations for sediment transport are created assuming that the main hydraulic variables may be used to calculate the sediment transport rate. When using such equations for flow conditions other than those they were developed, compatibility is frequently poor due to the inconsistent nature of the underlying assumptions[8,9].

This research aims to quantify the total sediment transport rate of the Euphrates River in the upstream Ramadi Barrage, in addition to other hydraulic characteristics, and to select the most effective prediction model for this rate from among including Yang, Shen, Hung, Ackers, and White, Engelund and Hansen, and Bagnold's and Toffaleti's. A major cause for concern is the ongoing process of erosion and sedimentation along the Euphrates River in the study area, especially following each release of large flows from Haditha Dam upstream in the study area. The numerous commercial and industrial buildings developed along the river's banks will be influenced in some way by transportation, sedimentation, and erosion of sediments. Because the geomorphological dynamics of the river basin directly affect the processes of erosion, sedimentation, and transportation that take place in the River path, it is necessary to improve our understanding of the mechanisms of sediment transport and management as well as the equations that can be applied with tolerable accuracy to obtain satisfactory results.

2. STUDY AREA

Ramadi is a city in central Iraq, about 110 km west of Baghdad(Latitude: 33° 26' 40" N, Longitude: 43° 15' 44" E), as shown in Figure 1. It is the governorate's capital and the largest city and borders Jordan, Syria, and Saudi Arabia. The Ramadi city extends along the Euphrates. Ramadi is located in a very strategic location on the Euphrates and the route into Syria and Jordan to the west. Due to its status as a major hub for trade and transportation, the city has experienced substantial economic growth. This investigation focuses on the part of the Euphrates River in the upstream Ramadi Barrage. The diversion dam's northern and southern sections, known as Ramadi Barrage, were built on the Euphrates River in the 1950s. The main job of the north of Barrage is to raise the river's water level if needed so that water can flow through the southern Barrage [10, 11,12]. The Euphrates is controlled by the Warrar Regulator, which dumps extra floodwater into Habbaniyeh Lake. The Barrage has 24 apertures, each measuring 6 by 8 meters, and is made of concrete. Its iron gates can be raised and lowered manually or electronically. The Barrage's ship channel and fish ladder are 6 meters wide and 40 meters long. A 7 m wide bridge has been constructed over the Barrage to accommodate large vehicles. At an elevation of 51.50 meters above sea level, the Barrage is designed to have a discharge of 3600 m^3/s. On the upstream left is the Warrar Regulator, composed of 24 gates with dimensions of (6×8) m. The maximum discharge of the regulator is 2800 m^3/s[13, 14, 15]. There is an urgent need to determine how much sediment transport is transmitted via this portion of the river and to come up with remedies because the sand islands and sedimentation in front of the upstream Ramadi Barrage have become an issue[16].

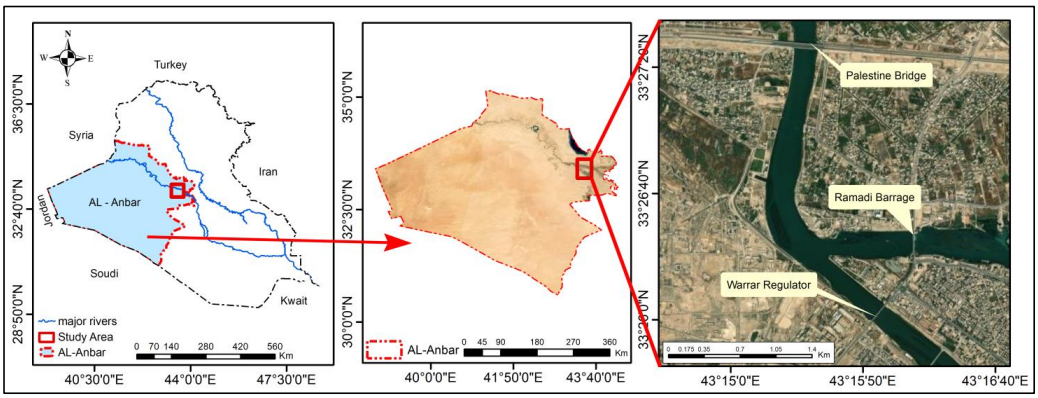

Figure 1: The study area.

3. MATERIALS AND METHODS

3.1. Field Measurements

The total sediment discharge is the total volume of sediment particles in motion over time. It includes the sediment transfer by bed load motion, the suspended load, and the wash load [17]. Bed load refers to sediment in almost continuous contact with the bed, carried forward by rolling, sliding, or hopping. The bed load creation process begins when the flow velocity increases to a point where the material may be detached and moved from its initial position. The particles will continue to move If the hydrodynamic force is sufficient to maintain the transportation. Furthermore, as soon as the hydrodynamic forces are reduced to the point where they can no longer move the particles, the sediment particles will cease moving and come to rest [18,19]. The majority of the wash load material in the Euphrates River within the study area originates from surface runoff following the intense rainstorms that fall on the catchments in the desert upstream of the study area. Any rainfall did not precede the days during which the sediment samples were taken; therefore, no washing load material is expected among the suspended load materials. Because the study area is in an arid region and the river's flow is controlled by the Haditha dam, which is located about 150 km upstream of the study reach and traps the wash load of the river. Either directly or indirectly, it is possible to estimate the amount of sediment that passes through a section. The direct method seeks to calculate the volume or weight of sediment that passes through a section over time [20]. The fieldwork aims to collect the necessary data such as suspended load, bedload, the particle size of the bed material, flow rate, water temperature, the river's width, water depth, and the level of the Euphrates River upstream of Ramadi Barrage in Anbar. The total river width (W) was divided into five vertical widths (Wi) [21].

The location of the measurement point is in the middle distance for each of the five verticals. The bed load transport is measured using the BLS30 bed load sampling instrument, as shown in Figure 2. Measured bed load movement for a period of (30 minutes) at each measurement sample. The suspended sediment was quantified Using a depth-integrated suspended sediment sampler Figure 3. The filling rate is intended to be proportional to the flow rate to depict the average concentration and particle size in each vertical. For this study, there are (350) samples of bed load and (350) samples of suspended load taken from the study area's cross-section. Bed load sampling, the suspended load, and the hydraulic parameters, such as flow depth and

velocity, are simultaneously measured at every vertical section. The Euphrates River's longitudinal slope in the study area was calculated to be 0.0001[22,23].

Figure 2: Bed load sampler BLS30 in the study area.

Figure 3: Depth-integrating suspended sediment sampler.

The bed load transmission rate for the measured cross-section is calculated using the equations below [24].

$$\mathbf{Q_B} = \sum_{\mathbf{i=1}}^{\mathbf{n-1}} \mathbf{W_i} \times \left(\frac{\mathbf{R_i + R_{i+1}}}{\mathbf{2}}\right) \quad (1)$$

$$\mathbf{R_i} = \frac{\mathbf{M}}{\mathbf{N_S \times t}} \quad (2)$$

The concentration of suspended sediment was calculated using the following Equation.

$$\text{Sediment Concentration } \boldsymbol{C_s} = \frac{\boldsymbol{Mass\ of\ Sediment(M)}}{\boldsymbol{Volume\ of\ Water\ (V)}} \quad (3)$$

Where C_s is concentration in mg/L; M is mass in mg; V is the volume in liter.

The grain size distribution is one of the most important characteristics of sediments. A soil sample's (soil particle gradation) river bed's particle size analysis aims to identify the relative characteristics of the various grain sizes that make up the sample. A stainless steel Van Veen Grab instrument was used for sampling the river bed, as shown in Figure 4. Van Veen Grab. The particle distribution curve was plotted after the bed material's particle size was measured by sieve analysis in the laboratory. The particle size distribution curve is displayed in Figure 5.

Figure 4: Van Veen Grab device.

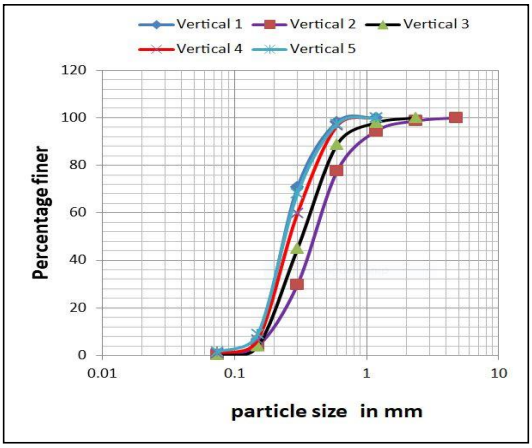

Figure 5: Particle size distribution curve.

Table 1: Summary of field and laboratory measurements.

n	Month	Bed load (g/30 min)					The concentration of suspended load (g/L)					Average velocity (m/s)	Depth (m)	Water Temp. (℃)
		V1	V2	V3	V4	V5	V1	V2	V3	V4	V5			
1	Jun. 2022	129.8	594.9	252.1	803.4	13.0	0.113	0.138	0.125	0.131	0.119	0.390	4.0	28.4
2	Jun. 2022	7.1	164.0	297.6	174.6	15.0	0.131	0.125	0.163	0.150	0.094	0.362	4.04	27.9
3	Jun. 2022	227.7	14.2	618.1	105.2	22.1	0.113	0.131	0.144	0.138	0.125	0.400	3.84	28.4
4	Jun. 2022	61.3	123.6	240.9	434.9	8.5	0.119	0.138	0.138	0.144	0.106	0.434	3.86	28.9
5	Jun. 2022	12.8	525.5	322.8	681.5	366.4	0.100	0.138	0.144	0.131	0.094	0.391	4.02	29.6
6	Jun. 2022	278.0	140.1	308.0	204.0	5.4	0.106	0.131	0.131	0.144	0.131	0.339	3.9	29.3
7	Jun. 2022	87.0	191.9	18.1	740.2	51.6	0.094	0.088	0.131	0.150	0.119	0.387	4.16	28.9
8	Jun. 2022	340.0	298.1	4.1	72.0	66.8	0.094	0.094	0.119	0.125	0.100	0.436	3.98	29.6
9	Jun. 2022	234.4	216.0	640.7	16.4	178.6	0.106	0.100	0.125	0.125	0.094	0.401	4.08	29.8
10	Jun. 2022	147.4	249.5	8.3	223.4	39.1	0.088	0.100	0.131	0.138	0.094	0.403	4.04	30.1
11	Jun. 2022	148.0	330.5	434.6	386.1	6.7	0.106	0.113	0.125	0.138	0.100	0.404	4.06	30.4
12	Jun. 2022	234.1	182.4	240.9	142.3	19.1	0.131	0.131	0.138	0.144	0.081	0.398	4.06	29.3
13	Jun. 2022	1.4	75.7	148.0	572.1	40.3	0.094	0.119	0.138	0.113	0.088	0.417	4.04	30.2
14	Jun. 2022	8.5	75.8	124.5	249.5	149.0	0.100	0.125	0.131	0.144	0.113	0.376	4.16	30.9
15	Jul. 2022	24.2	71.3	75.5	417.9	219.3	0.094	0.106	0.125	0.125	0.088	0.361	4.02	31.6
16	Jul. 2022	194.3	179.3	124.2	405.9	3.8	0.100	0.113	0.113	0.119	0.094	0.381	4.06	31.8
17	Jul. 2022	636.7	282.5	456.9	17.5	139.7	0.113	0.131	0.088	0.119	0.119	0.397	4.14	30.8
18	Jul. 2022	884.0	241.5	622.5	729.6	28.9	0.125	0.138	0.150	0.119	0.131	0.408	4.2	31.6
19	Jul. 2022	644.4	67.1	317.0	164.9	41.0	0.131	0.144	0.138	0.125	0.125	0.406	4.02	32.2
20	Jul. 2022	634.7	187.2	510.3	440.3	65.0	0.113	0.156	0.144	0.125	0.106	0.434	3.94	32.3
21	Jul. 2022	233.2	98.2	408.0	320.1	124.6	0.119	0.131	0.163	0.131	0.138	0.392	4.14	31.9
22	Jul. 2022	19.4	317.3	241.2	79.4	29.0	0.113	0.131	0.131	0.156	0.144	0.398	4.08	30.8
23	Jul. 2022	67.4	822.5	364.7	432.6	8.1	0.125	0.131	0.150	0.144	0.094	0.400	4.08	32.0
24	Jul. 2022	26.7	228.7	435.9	372.7	9.3	0.131	0.088	0.144	0.113	0.119	0.431	4.0	31.6
25	Jul. 2022	148.6	434.7	568.7	388.6	162.7	0.094	0.138	0.138	0.125	0.088	0.424	3.72	30.4
26	Jul. 2022	38.5	5.3	378.7	436.7	128.7	0.106	0.119	0.138	0.131	0.088	0.416	4.04	30.9
27	Jul. 2022	122.7	74.4	314.3	196.3	32.8	0.113	0.131	0.144	0.138	0.100	0.403	3.94	31.0
28	Jul. 2022	38.7	248.3	178.7	202.5	6.5	0.131	0.125	0.125	0.138	0.081	0.384	3.88	32.4
29	Aug. 2022	218.6	28.6	240.5	817.0	7.0	0.131	0.131	0.125	0.138	0.119	0.431	3.86	30.5
30	Aug. 2022	79.3	5.8	262.0	588.8	33.8	0.106	0.125	0.131	0.138	0.094	0.390	4.02	30.43
31	Aug. 2022	34.5	238.7	266.2	380.0	122.5	0.131	0.138	0.138	0.150	0.125	0.470	3.84	30.0
32	Aug. 2022	174.2	234.3	190.0	622.8	26.0	0.125	0.131	0.138	0.131	0.131	0.434	3.9	30.0
33	Aug. 2022	224.0	188.6	235.3	267.3	4.1	0.125	0.144	0.138	0.144	0.131	0.419	4.02	30.4
34	Aug. 2022	47.6	220.0	192.9	168.3	38.6	0.131	0.125	0.144	0.138	0.131	0.439	4.06	30.5
35	Aug. 2022	294.7	243.6	422.7	374.9	82.5	0.119	0.156	0.131	0.138	0.138	0.404	4.06	29.8
36	Aug. 2022	178.2	284.6	386.5	528.7	194.5	0.125	0.131	0.138	0.150	0.131	0.406	4.06	29.7
37	Aug. 2022	196.9	235.2	592.6	332.2	62.1	0.125	0.138	0.150	0.138	0.094	0.427	4.1	30.7
38	Aug. 2022	122.1	214.7	439.5	392.7	28.7	0.138	0.138	0.169	0.144	0.131	0.439	4.08	30.1
39	Aug. 2022	36.7	138.1	333.9	302.4	58.7	0.125	0.150	0.163	0.156	0.131	0.431	4.02	30.8
40	Aug. 2022	528.7	324.2	542.8	240.7	23.9	0.119	0.138	0.131	0.144	0.119	0.421	4.02	31.0
41	Aug. 2022	368.8	128.8	382.9	264.5	79.6	0.125	0.138	0.144	0.138	0.131	0.439	3.96	31.1
42	Aug. 2022	58.5	247.1	408.3	296.7	12.4	0.113	0.131	0.150	0.144	0.125	0.435	3.98	31.0
43	Sep. 2022	314.0	282.8	422.7	250.9	187.3	0.144	0.144	0.138	0.131	0.131	0.426	4.04	29.8
44	Sep. 2022	440.7	243.3	522.7	448.7	132.3	0.119	0.138	0.138	0.131	0.125	0.439	3.92	29.7
45	Sep. 2022	22.7	247.3	353.7	368.7	35.2	0.131	0.131	0.150	0.138	0.131	0.424	3.78	29.7
46	Sep. 2022	167.1	345.7	332.7	168.5	214.2	0.125	0.138	0.144	0.138	0.113	0.412	3.94	29.1
47	Sep. 2022	28.7	273.0	348.4	247.3	148.7	0.106	0.131	0.144	0.125	0.119	0.369	4.04	28.7
48	Sep. 2022	192.3	197.5	218.5	172.7	72.5	0.131	0.125	0.138	0.138	0.100	0.406	3.96	28.3
49	Sep. 2022	169.4	384.2	508.9	270.9	82.0	0.125	0.131	0.138	0.138	0.113	0.409	3.92	28.0
50	Sep. 2022	228.5	178.0	246.2	128.5	42.3	0.094	0.131	0.125	0.125	0.094	0.422	4.0	28.0
51	Sep. 2022	258.7	148.7	428.3	165.5	262.5	0.125	0.138	0.138	0.125	0.131	0.425	3.92	27.6
52	Sep. 2022	158.1	344.7	368.5	174.7	248.4	0.131	0.125	0.131	0.138	0.119	0.404	3.96	27.4
53	Sep. 2022	224.4	388.5	579.2	418.6	130.0	0.138	0.144	0.150	0.131	0.131	0.388	4.06	27.6
54	Sep. 2022	125.6	252.5	428.7	371.3	40.0	0.119	0.125	0.131	0.138	0.113	0.441	3.9	27.8
55	Sep. 2022	196.7	98.2	294.7	171.3	247.3	0.138	0.131	0.150	0.138	0.131	0.438	3.92	27.0
56	Sep. 2022	77.9	207.3	122.1	207.4	132.6	0.125	0.125	0.138	0.131	0.125	0.417	3.88	27.6
57	Oct. 2022	160.4	233.1	296.8	374.6	110.8	0.131	0.125	0.131	0.138	0.119	0.379	4.08	27.1
58	Oct. 2022	98.6	251.7	338.8	402.7	67.3	0.125	0.150	0.138	0.138	0.131	0.423	4.08	27.0
59	Oct. 2022	34.7	228.1	269.3	242.4	78.3	0.131	0.131	0.138	0.131	0.119	0.436	4.06	27.3
60	Oct. 2022	141.3	195.7	254.7	159.8	8.6	0.131	0.125	0.144	0.150	0.125	0.393	3.98	26.4
61	Oct. 2022	32.1	322.7	232.4	260.1	24.9	0.125	0.131	0.138	0.144	0.100	0.432	3.98	26.92
62	Oct. 2022	42.0	172.3	208.4	188.7	26.1	0.131	0.131	0.144	0.138	0.113	0.414	4.04	26.4
63	Oct. 2022	63.5	214.6	264.0	223.8	36.3	0.125	0.131	0.150	0.138	0.106	0.428	3.88	26.3
64	Oct. 2022	240.6	188.0	434.7	298.0	46.3	0.131	0.138	0.156	0.144	0.125	0.408	3.9	26.9

Table 1: (Continued), Summary of field and laboratory measurements.

n	Month	Bed load (g/30 min)					The concentration of suspended load (g/L)					Average velocity (m/s)	Depth (m)	Water Temp. (°C)
		V1	V2	V3	V4	V5	V1	V2	V3	V4	V5			
65	Oct. 2022	158.3	87.3	388.6	236.2	102.9	0.125	0.144	0.150	0.144	0.131	0.412	3.98	26.8
66	Oct. 2022	222.6	122.3	480.7	417.5	19.3	0.138	0.163	0.163	0.150	0.138	0.437	3.96	25.6
67	Oct. 2022	196.9	228.5	264.2	243.7	67.3	0.144	0.144	0.150	0.138	0.131	0.434	3.8	25.8
68	Oct. 2022	148.4	179.2	290.4	188.2	16.8	0.125	0.150	0.156	0.144	0.138	0.432	3.94	25.9
69	Oct. 2022	231.1	254.2	526.0	402.8	48.2	0.113	0.144	0.150	0.150	0.138	0.419	3.98	25.5
70	Oct. 2022	168.3	175.3	340.7	248.9	122.4	0.131	0.150	0.138	0.150	0.100	0.450	4.0	25.4
Min.		1.4	5.3	4.1	16.4	3.8	0.088	0.088	0.088	0.113	0.081	0.339	3.720	25.5
Avg.		182.0	223.1	333.1	320.6	78.7	0.120	0.131	0.139	0.137	0.116	0.413	3.991	29.3
Max.		884.0	822.5	640.7	817.0	366.4	0.144	0.163	0.169	0.156	0.144	0.470	4.200	32.4

3.2 Sediment Transport Equations

The suspended and bed loads make up a river's total load. Most sediment transport equations are derived based on theoretical and empirical foundations. There isn't a universal formula that can be deemed suitable to determine a sediment transport rate for all rivers because these equations include a boundary condition and shouldn't be used as a general rule [25]. This justification points to the necessity for more research in this area. Some of the empirical equations used in this study to determine total loads are listed below. Yang's Equation [26].

$$\log C = 5.435 - 0.286 \log \frac{wd_{50}}{v} - 0.457 \log \frac{u_*}{w} + \left[1.799 - 0.409 log \frac{wd_{50}}{v} - 0.314 log \frac{u_*}{\omega}\right] \log \left[\frac{VS}{\omega} - \frac{V_{cr}S}{\omega}\right] \quad (4)$$

$$\frac{V_{cr}}{w} = \frac{2.5}{log\frac{u_* d_{50}}{v} - 0.06} + 0.66 \quad for\ 1.2 < \frac{u_* d_{50}}{v} < 70 \quad (5)$$

$$\frac{V_{cr}}{\omega} = 2.05 \quad for\ \frac{u_* d_{50}}{v} \geq 70 \quad (6)$$

In which C is the total concentration (mg/L); ω is the fall velocity; d_{50} is the particle size; v is the kinematic viscosity (ft^2/s); u_* is the shear velocity (fps); S is the slope (ft/ft); V is the mean velocity (fps); V_{cr} is the crucial flow velocity at the motion's beginning (fps); D is the water depth. Ackers and White (1973) [27].

$$x = \frac{G_{g_r} Gs\, d}{D\left(\frac{U_*}{V}\right)^n} \quad (7)$$

$$G_{g_r} = c\left(\frac{F_{gr}}{A} - 1\right)^m \quad (8)$$

In which G_{g_r} is the sediment transport parameter; d is the particle diameter average (m); D is the effective depth (m); V is the average velocity(m/s); n is the exponent of transition, which varies depending on the size of the sediment; C is the Coefficient; F_{gr} is the sediment mobility parameter; A is the crucial sediment mobility parameter; U_* is the shear velocity (m/s); Gs is the Sediment Specific Gravity; x is the sediment flow by fluid weight, in parts per million. Engelund and Hansen's [27].

$$q_s = 0.05 V^2 \gamma_s \sqrt{\frac{d_{50}}{g\left(\frac{\gamma_s}{\gamma} - 1\right)}} \left(\frac{\tau_\circ}{(\gamma s - \gamma) d_{50}}\right)^{1.5} \quad (9)$$

In which q_t is total sediment discharge in weight per unit width; S is the energy slope; V is the flow velocity; $\gamma_s and\ \gamma$ is the respective specific weights of sediment and water.; d_{50} is the median particle diameter; g is the gravitational acceleration; τ is the shear stress along the bed. Bagnold's Equation [27].

$$q_t = \frac{\gamma}{\gamma_s - \gamma} \tau V \left(\frac{e_b}{tan\alpha} + 0.01 \frac{V}{\omega}\right) \quad (10)$$

In which q_t is the total sediment transport rate by weight per unit channel width; γ_s, γ specific weight of sediment and water, respectively; $\tan\alpha$ is the ratio of tangential to normal shear force; τ is the shear force acting along the bed; V is the average flow velocity; e_b is the efficiency coefficient.

4. RESULTS AND DISCUSSION

In this study, Yang, Ackers and White, Engelund and Hansen, Shen and Hung, Bagnold, and Toffaleti equations were chosen to assess sediment transport in The Euphrates River. Table 2 summarizes the values for the measured and computed total load. For the analysis in the present study, various statistical measures are calculated to compare the performance of the selected equations, as discussed below. To assess the

applicability of sediment load equations. The discrepancy ratio (DR) is defined as the ratio of computed total load to measured total load. The discrepancy ratio is scheduled in the range (0.5-2) [28, 29]. The results are presented in Table 3. The deviation of predicted values from the observed values is obtained graphically utilizing sediment load equations, as shown in Figure 6.

Table 2. The total load calculated and measured

Vertical	Measured ton/day	Yang ton/day	Ackers and White ton/day	Engelund and Hansen ton/day	Shen and Hung ton/day	Bagnold ton/day	Toffaleti ton/day
V1	312.35	40.61	44.83	375.76	4.21	101.90	35.52
V2	762.16	150.49	112.34	752.69	18.76	189.89	34.50
V3	1516.13	388.61	327.75	2414.19	32.08	134.85	212.49
V4	1281.79	338.43	349.36	2304.01	78.39	361.58	218.54
V5	388.90	53.49	50.96	530.67	6.11	105.27	11.71

Table 3. Summary of accuracies of different formulas.

Formulas	Percentage of data in the range
Yang	11
Ackers and White	8
Engelund and Hansen	94
Shen and Hung	0
Bagnold	20
Toffaleti	0

The discrepancy ratio must be one to achieve a complete correlation between $\mathbf{q_c}$ and $\mathbf{q_m}$. To test the reliability of preliminary results obtained based on DR, further statistical measures like mean absolute percentage error (MAPE), root mean squared error (RMSE), and scatter index (SI) were calculated and compared. These statistical measures are calculated as given by Equations 12 and 13. The standard deviation is calculated using Equation 14, and the averaged variation coefficient is calculated using Equation 15. Table 4 presents the results of statistical measures and correlations of computed and observed sediment load transport.

$$DR=\frac{q_c}{q_m} \tag{11}$$

$$RMSE=\sqrt{\frac{\sum_{i=1}^{n}(TL_o-TL_c)^2}{N}} \tag{12}$$

$$SI=\frac{\sqrt{\frac{1}{n}\sum_{i=1}^{n}((TL_p-\overline{TL_p})-(TL_o-\overline{TL_o}))^2}}{\frac{1}{n}\sum_{i=1}^{n}TL_o} \tag{13}$$

$$\sigma=\sqrt{\sum_{i=1}^{n}(DR-\overline{V_c})^2/(n-1)} \tag{14}$$

$$\overline{V_c}=\sum_{i=1}^{n}\frac{DR}{n} \tag{15}$$

Where q_m is the measured sediment discharge and q_c is the computed value, TL_p is the predicted total load, $\overline{TL_p}$ is the mean predicted total load, TL_o is observed total load, $\overline{TL_o}$ is the mean observed total load, and n is the total number of observations.

Table 4. Comparison using statistical methods

Formula	SI	RMSE	Average of variation coefficient	The standard deviation of the variation coefficient
Yang	0.16	675	0.19	0.076
Ackers and White	0.15	691	0.17	0.095
Engelund and Hansen	0.37	496	1.36	0.386
Shen and Hung	0.18	854	0.01	0.013
Bagnold	0.17	692	0.24	0.088
Toffaleti	0.16	771	0.09	0.087

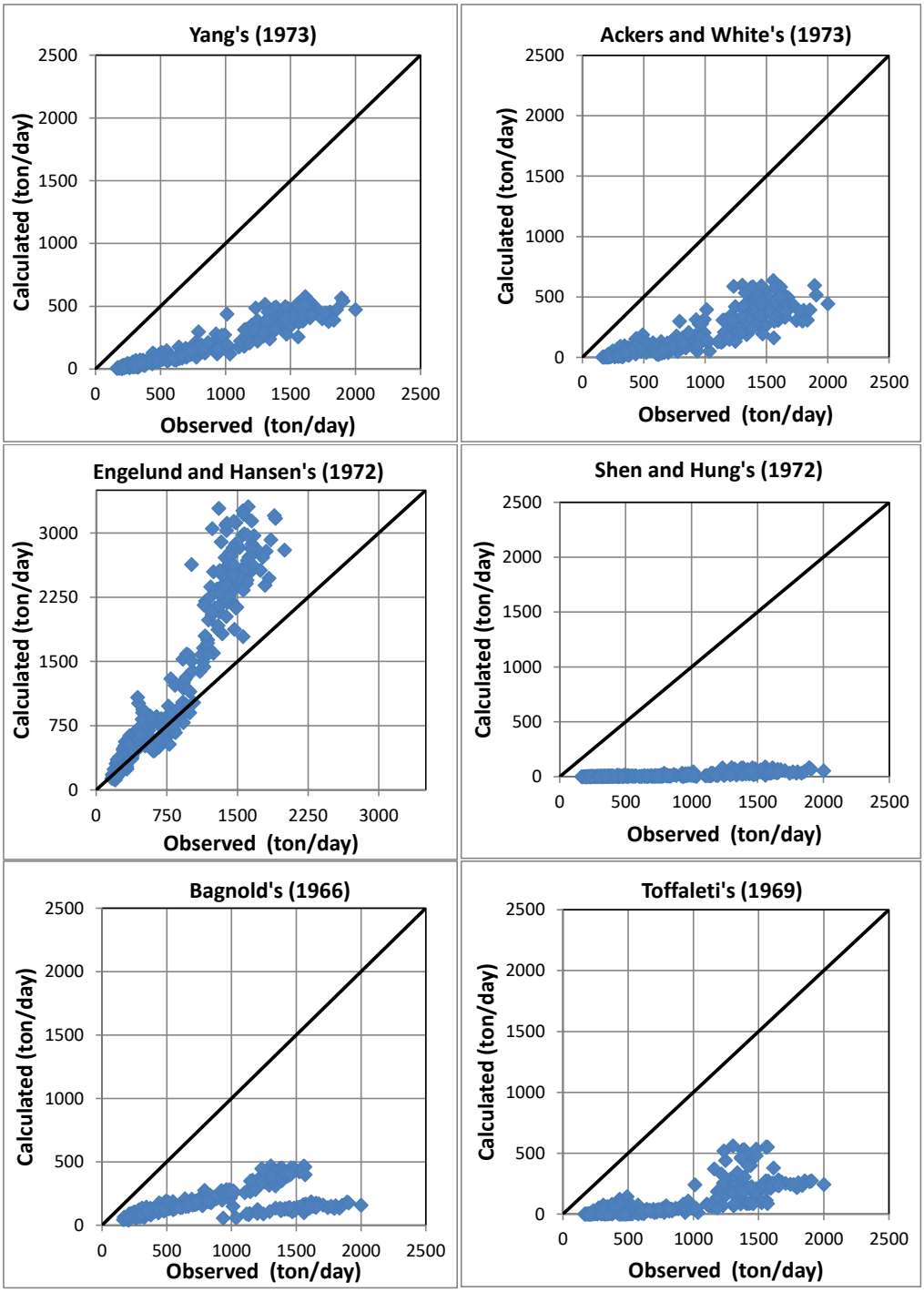

Figure 6. Total load rate calculated and observed.

The results given by the various formulas are different, and there is very poor agreement between them. The large deviation between measured sediment transport and calculated is a consequence of each Equation being derived under conditions specific to each study area and cannot be applied to other study areas with conditions different from the conditions from which these equations were derived. This illustrates how specific the presumptions underlying these calculations are. From statistical measures and graphical comparison, it can be said that the Englund and Hansen equation gives more reliable results than the other equations used

in this study, as shown in Figure 6, to estimate the amount of sediment transported in the Euphrates River upstream of Ramadi Barrage in Iraq.

Numerous academics discussed the likely causes of variations in the sediment load projected by different formulas. This variation in the forecast can be explained by the irrational behavior of some relevant factors, including flow velocity, fall velocity, shear stress, particle exposure, etc. Another element that requires more research is the impact of turbulence on the bed load transport separation of the flow across the bed forms, which also contributes to the turbulence[30, 31]. It is believed that the presence of surface organization such as clusters, imbrications, or protuberant clast may act as a source or sink to incoming sediment particles[32]. Most existing formulas for sediment transport were developed with the idea that stream characteristics like velocity, boundary shear stress, etc., could adequately describe sediment transport, while vertical elements like water depth (pressure) variance across time and space were left out[33]. One further crucial element is bed shape, which directly impacts other random characteristics and can result in an entirely different scenario[34].

5. CONCLUSIONS

The current study aimed to determine how well some empirical equations may be used to predict sediment flow. Given the absence of measurement processes in the study area, it is crucial to specify the sediment transport equations that can be used to obtain satisfactory results for monitoring the erosion, sedimentation, and transport processes. This will save time and effort when evaluating and monitoring the processes of erosion and sedimentation. Used various empirical formulas, including Yang, Ackers, and White, Engelund and Hansen, Shen and Hung, Bagnold's, and Toffaleti's methods. According to the results obtained by this study, the following conclusions may be drawn:

- The average total sediment rate in the study is 4267.60 tonnes/day.
- The particle size of bed load material analysis showed that the Euphrates River bed load comprises 100% sand in the study area.
- The Engelund and Hansen (1967) model is the most appropriate from a practical engineering standpoint when considering hydraulic design and sustainability for this site from the river.

REFERENCES

[1] Rice SK. Suspended Sediment Transport In The Ganges-Brahmaputra River System, Bangladesh. Ятыатат [Internet]. 2007;вы12у(235):245.
[2] Mustafa AS, Sulaiman SO, Al_Alwani KM. Application of HEC-RAS Model to Predict Sediment Transport for Euphrates River from Haditha to Heet 2016. J Eng Sci. 2017;20(3):570–7.
[3] Sulaiman SO, Al-Ansari N, Shahadha A, Ismaeel R, Mohammad S. Evaluation of sediment transport empirical equations: case study of the Euphrates River West Iraq. Arab J Geosci. 2021;14(10).
[4] Salih SQ, Sharafati A, Khosravi K, Faris H, Kisi O, Tao H, et al. River suspended sediment load prediction based on river discharge information: application of newly developed data mining models. Hydrol Sci J. 2020;65(4):624–37.
[5] Yadav SM, Yadav VK, Gilitwala A. Evaluation of bed load equations using field measured bed load and bed material load. ISH J Hydraul Eng [Internet]. 2021;27(S1):113–23. Available from: https://doi.org/10.1080/09715010.2019.1594417
[6] Aude SA, Mahmood NS, Sulaiman SO, Abdullah HH, Al Ansari N. Slope Stability and Soil Liquefaction Analysis of Earth Dams With a Proposed Method of Geotextile Reinforcement. Int J GEOMATE. 2022;22(94):102–12.
[7] Tao H, Keshtegar B, Yaseen ZM. The feasibility of integrative radial basis M5Tree predictive model for river suspended sediment load simulation. Water Resour Manag. 2019;33(13):4471–90.
[8] Afan HA, El-shafie A, Mohtar WHMW, Yaseen ZM. Past, present and prospect of an Artificial Intelligence (AI) based model for sediment transport prediction. J Hydrol. 2016;541:902–13.
[9] Sharafati A, Haghbin M, Motta D, Yaseen ZM. The application of soft computing models and empirical formulations for hydraulic structure scouring depth simulation: a comprehensive review, assessment and possible future research direction. Arch Comput Methods Eng. 2021;28(2):423–47.
[10] Abdulhameed IM, Sulaiman SO, Najm ABA. Reuse Wastewater by Using Water Evaluation and Planning (WEAP) (Ramadi City-Case Study). IOP Conf Ser Earth Environ Sci. 2021;779(1).
[11] Noon AM, Ahmed HGI, Sulaiman SO. Assessment of water demand in Al-Anbar province- Iraq. Environ Ecol Res. 2021;9(2):64–75.
[12] Kosaj R, Alboresha RS, Sulaiman SO. Comparison between Numerical Flow3d Software and Laboratory Data, for Sediment Incipient Motion. IOP Conf Ser Earth Environ Sci. 2022;961(1).
[13] Sayl KN, Sulaiman SO, Kamel AH, Muhammad NS, Abdullah J, Al-Ansari N. Minimizing the Impacts of Desertification in an Arid Region: A Case Study of the West Desert of Iraq. Adv Civ Eng. 2021;2021(June 2009).

[14] Sulaiman SO, Kamel AH, Sayl KN, Alfadhel MY. Water resources management and sustainability over the Western desert of Iraq. Environ Earth Sci [Internet]. 2019;78(16):1–15. Available from: https://doi.org/10.1007/s12665-019-8510-y
[15] Sulaiman SO, Rajaa AI. Cost-benefit analysis of suggested Ramadi Barrage hydroelectric plant on the Euphrates River. Int J Comput Aided Eng Technol. 2022;17(1):34–44.
[16] Mahmood NS, Aude SA, Abdullah HH, Sulaiman SO, Ansari N Al. Analysis of Slope Stability and Soil Liquefaction of Zoned Earth Dams Using Numerical Modeling. Int J Des Nat Ecodynamics. 2022;17(4):557–62.
[17] Weber LJ. The Hydraulics of Open Channel Flow: An Introduction. J Hydraul Eng. 2004;127(3):246–7.
[18] Hassan AO, Mohammed YF, Sadiq QS. A model for removing sediments from open channels. Int J Phys Sci. 2014;9(4):61–70.
[19] van Rijn L. SEDIMENT TRANSPORT, Part I: Bed load transport. J Hydraul Eng. 1984;110(10):1431–56.
[20] Addab H, Al-Saadi SIK. Estimation of Sediment Quantity of the Al-Meshkab Regulator Channel. Kufa University; 2011.
[21] Manual R. Volume 5 sediment transport measurements. 2003;5.
[22] Mhmood HH, Yilmaz M, Sulaiman SO. Simulation of the flood wave caused by hypothetical failure of the Haditha Dam. Journal of Applied Water Engineering and Research. 2022.
[23] Sulaiman SO, Najm ABA, Kamel AH, Al-Ansari N. Evaluate the optimal future demand of water consumption in Al-Anbar province in the west of Iraq. Int J Sustain Dev Plan. 2021;16(3):457–62.
[24] Sun Z, Donahue J. Statistically derived bedload formula for any fraction of nonuniform sediment. J Hydraul Eng. 2000;126(2):105–11.
[25] Bunte K, Abt SR, Potyondy JP, Ryan SE. Measurement of coarse gravel and cobble transport using portable bedload traps. J Hydraul Eng Vol 130, no 9 (Sept 2004) p 879-893. 2004;
[26] Yang CT, Molinas A. Sediment transport and unit stream power function. J Hydraul Div. 1982;108(6):774–93.
[27] Yang CT. Sediment Transport. 1996.
[28] Khassaf SI, Safaa K.Hashim A, Sharba NM. Development of New Formula for Computing Total Sediment Loads at Upstream of AlShamia Barrage. 2016;1(November):1–8.
[29] Khassaf SI, Jaber Abbas M. Modeling of Sediment Transport Upstream of Al-Shamia Barrage. 2015;
[30] Nakagawa H, Zhang H. Modeling of Total Sediment Load Transport in Alluvial Rivers. Proc Hydraul Eng. 2004;48:931–6.
[31] Isabel L, Ramon L. 2D numerical modelling of sediment transport with non uniform material. 2013;(June):1–103.
[32] Zaidan K, Khassaf SI. Sediment Transport Upstream of Reservoir of Haditha Dam. J Eng Dev Vol 9, No 4, 2005. 2005;(December 2005).
[33] Al-Ansari NA, Asaad NM, Walling DE, Hussan SA. The suspended sediment discharge of the river Euphrates at Haditha, Iraq: an assessment of the potential for establishing sediment rating curves. Geogr Ann Ser A, Phys Geogr. 1988;70(3):203–13.
[34] Gomez B, Church M. An assessment of bed load sediment transport formulae for gravel bed rivers. Water Resour Res. 1989;25(6):1161–86.